Journal of Physics: Conference Series **190** (2009) 012047 doi:10.1088/1742-6596/190/1/012047

Orientation-dependent x-ray Raman scattering from cubic crystals: natural linear dichroism in MnO and CeO_2

R A Gordon[1], M W Haverkort[2], Subhra Sen Gupta[3] and G A Sawatzky[3]

[1] Dept. of Physics, Simon Fraser University, Burnaby, BC V5A 1S6 Canada
[2] Max Planck Institute for Solid State Research, Heisenbergstr. 1, 70506 Stuttgart, Germany
[3] Dept. of Physics and Astronomy, University of British Columbia, Vancouver, BC V6T 1Z1 Canada

E-mail: ragordon@sfu.ca

Abstract. Information on valence orbitals and electronic interactions in single crystal systems can be obtained through orientation-dependent x-ray measurements, but this can be problematic for a cubic system. Polarisation-dependent x-ray absorption measurements are common, but are dominated by dipole transitions which, for a cubic system, are isotropic even though a cubic system is not. Many edges, particularly for transition metals, do have electric quadrupole features that could lead to dichroism but proximity to the dipole transition can make interpretation challenging. X-ray Raman Spectroscopy (XRS) can also be used to perform orientation-dependent near-edge measurements - not only dependent on the direction of the momentum transfer but also its magnitude, q. Previous XRS measurements on polycrystalline materials revealed that multipole (higher order than dipole) transitions are readily observable in the pre-threshold region of rare earth $N_{4,5}$ edges, actually replacing the dipole at high-q. We have extended these studies to examine orientation-dependent XRS for CeO_2 and MnO single crystals, as prototype systems for theoretical treatment. Dichroism is observed at both the Ce $N_{4,5}$ and Mn $M_{2,3}$ edges in these cubic materials.

1. Introduction

The arrangement of atoms in a crystal is never isotropic. The resulting anisotropy in charge distribution about a target atom – the local Crystal Field (CF) – affects the electronic structure of the atom. When examining the electronic structure of a target atom in a single crystal with an orientation-sensitive technique such as x-ray absorption using a linearly polarized x-ray beam, or x-ray scattering with scattering vector along different crystallographic directions, the resultant measurements may exhibit an orientation-dependence – natural dichroism – as a consequence of the character of the target and its interaction with the CF [1-6].

The ability to measure dichroism is dependent on the symmetry of the crystal system and the type of transition involved. Absorption-based measurements like X-ray Absorption Near-Edge Structure (XANES) or Resonant Inelastic X-ray Scattering (RIXS, and the related Resonant X-ray Emission Spectroscopy, RXES) are dominated by dipole transitions. The dipole transition cannot distinguish a symmetry involving a higher-than-2-fold axis from spherical symmetry and so, cannot see anisotropic charge distributions in many crystal systems with high symmetry such as cubic. The absorption process being dominated by dipole behavior does not preclude the existence of higher-order (e.g.

quadrupole) features in the near-edge region. Transition metal (3d) K-edges can possess pre-edge features with 3d character that may be purely quadrupole (1s – 3d) or dipole due to 3d - 4p mixing, and have been studied extensively for their sensitivity to local environment and speciation [7]. Examination of these pre-K-edge features for dichroism has met with some success, even in cubic systems [5, 6]. RIXS measurements have also revealed quadrupole *d-d* transitions that are sensitive to orientation [8, 9]. The presence of quadrupole features in L-edge spectra of some rare earth materials [10] suggests that such non-dipole features could be similarly used to examine natural dichroism in high-symmetry rare-earth-containing crystals. These techniques however, being tied to the dipole resonance, generally, have no control as to the extent of non-dipole character present in the measured spectrum, though the quadrupole component can be enhanced using Borrmann methods [11].

Non-dipole features can be systematically observed using x-ray Raman spectroscopy (XRS) (i.e. non-resonant inelastic x-ray scattering (NIXS)). XRS provides an approach, complementary to soft x-ray absorption, to examine low energy valence-valence excitations and core-valence transitions in light and heavy element-containing compounds, but with hard x-rays (~10 keV), guaranteeing bulk sensitivity. Orientation and momentum-transfer (q) dependence of *d-d* excitations in NiO and CoO have been measured and modeled [12, 13]. Momentum-transfer-dependent multipole features in La and Ce-containing materials have been studied [14].

The dynamic structure factor for such a measurement is given [15] by:

$$S(\mathbf{q},\omega) = \sum_f |\langle f \mid e^{i\mathbf{q}\bullet\mathbf{r}} \mid i \rangle|^2 \, \delta(E_i - E_f + \hbar\omega) \qquad (1)$$

where the energy transfer between the initial and final states of the atom is ħω and **q**, the momentum transfer to the atom. Experimentally one has incident and outgoing x-ray energies, hν. Thus, ħω is also the x-ray energy loss, $h\nu_{in}$ - $h\nu_o$. At low q ($|\mathbf{q}|$), the expression reduces to a form similar to that for absorption, with **q** playing the role of polarization. With increasing q, one enters a regime where the dipole transition is suppressed and higher order terms dominate the spectrum. This is illustrated in figure 1 for a powder sample of CeO_2 with ħω comparable to the cerium $N_{4,5}$ absorption edge [14].

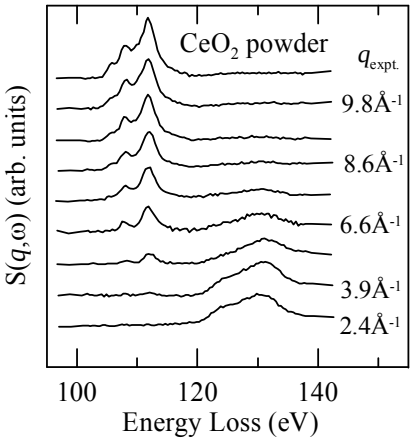

Figure 1. Contribution to S(q, ω) from the 4d initial states for a powder sample of CeO_2 measured with 1.5 eV energy resolution showing the effect of increasing momentum transfer on the XRS spectrum.

At low magnitude momentum transfer, a dipole-resonance feature is observed, similar to absorption measurements at the Ce $N_{4,5}$ edge. With increasing q, the dipole (2^1-pole) feature diminishes, while features first from an octupole (2^3-pole) and then a triakontadipole (2^5-pole) term contribute to a pre-threshold atomic-like multiplet spectrum at lower energy loss. Since these multiplet features (and, as will be shown below, related features for the Mn $M_{2,3}$ edges) are located significantly lower in energy than the dipole transition, they are less likely to be interacting with continuum states and may provide a clearer interpretation of the local electronic ground state than dipole-related transitions. Measurements and modeling of such non-dipole multiplet features for single crystal materials may provide insight on the influence of the CF on 3d or 4f elements, even in cubic (O_h) systems. We test

the feasibility of such studies by examining the high-q XRS directional-dependence of two cubic materials: MnO and CeO_2.

2. Experimental

Commercial substrates of manganese monoxide (manganosite) and cerium dioxide were obtained with the orientations: MnO – (100) and (111) (MaTecK/Princeton Scientific); CeO_2 – (100), (110) and (111) (Commercial Crystal Labs.). A powder sample of MnO [16] was also examined as a pressed-pellet. The CeO_2 crystals were black in colour as purchased and given a heat treatment to improve the oxygen content. They were heated in air up to 800 °C over a 24 hour period, held at this temperature for 1 hour, then cooled to room temperature over another 24 hour period. The slow heating and cooling profiles were necessary to protect the crystal integrity against stresses caused by changes in the lattice during oxygenation. After the heat treatment, the crystals were a translucent tan/orange colour similar to the commercial powder measured previously.

XRS measurements were made using the LERIX endstation at the PNC/XOR undulator beamline, 20ID, at the Advanced Photon Source [17]. While LERIX is normally equipped with 19 spherically-bent Si(111) analyzers, for these measurements, 4 diced analyzers were installed for improved resolution at select q values up to 10.1 $Å^{-1}$. Using a liquid-nitrogen-cooled Si(311) double-crystal monochromator and toroidal focusing of the monochromatic beam, the diced analyzers provided a resolution of 0.55 – 0.65 eV based on the full-width-half-max of the elastic peak for the 555-analyzer reflection near 9890 eV. The bent analyzers gave ~0.9 eV. Energy calibration was monitored by measuring the elastically-scattered peak before and after the edge scans. Room-temperature measurements near the Mn $M_{2,3}$ and Ce $N_{4,5}$ contributions to the scattering were done by scanning the monochromator energy above 9890 eV and monitoring the intensity reflected from the analyzer. Energy loss was obtained by subtracting the average elastic peak position from the scanned energy. Elastic peak positions varied by 0.08 eV at worst, with 0.02 eV typical, leading to a possible error in the positions of features of +/- 0.04 eV, and some additional broadening. Data for display is an average of 5 to 12 scans and has undergone a polynomial background removal and normalization to unit area.

3. Results and Discussion

Cubic MnO and CeO_2 crystallize in the NaCl and CaF_2 structure-types, respectively. Both cations (formal charge) are octahedrally coordinated by oxygen: Mn^{2+} by 6 O^{2-} ; and Ce^{4+} by 8 O^{2-}. Initial modelling treats an ionic cluster MnO_6^{10-} or CeO_8^{12-} using a local many-body approach within a configuration interaction cluster calculation. The exponential term in equation (1) is expanded [13, 14] in spherical harmonics to give:

$$e^{i\mathbf{q}\bullet\mathbf{r}} = \sum_{k=0}^{\infty}\sum_{m=-k}^{k} i^k (2k+1)\, j_k(qr) C_m^{(k)*}(\theta_q,\varphi_q) C_m^{(k)}(\theta_r,\varphi_r) \qquad (2)$$

with $C_m^{(k)} = (4\pi/(2k+1))^{1/2} Y_{km}$, $Y_{km}(\theta,\varphi)$ the spherical harmonics incorporating the orientation-dependence, and $j_k(qr)$ a spherical Bessel function of order, k. Note, for the integral in (1) to be non-vanishing, the combined angular momenta of the initial state, final state and transition operator must be zero. With the d-wavefunctions being even functions, and the p or f wavefunctions being odd functions, for transitions p-state to d-state or d-state to f-state, only the odd-k terms in (2), limited by the sum and difference of the angular momenta of the final (d or f) and initial (p or d) states, give non-zero results. This is similar to the treatment given by Haverkort *et al.* for NiO and CoO [13] *d-d* excitations, but including core hole effects owing to the core-valence transitions being examined. Radial expectation values for the allowed 2^k-pole terms (k=1, 3 for Mn 3p – 3d; k = 1, 3, 5 for Ce 4d – 4f) showing their q-dependence are given in that work.

Both these systems have, when considering formal charge, spherically symmetric initial states: $3p^6 3d^5$ (^6S) for Mn^{2+} and $4d^{10} 4f^0$ (^1S) for Ce^{4+}. In cubic (O_h) symmetry, the dipole (k=1) transitions transform under T_{1u}; the octupole (k=3) as A_{2u}, T_{1u} and T_{2u}; and the triakontadipole (k=5) as E_u, T_{1u},

T_{1u} and T_{2u}, respectively [18]. There is then one fundamental dipole contribution, three octupole and four triakontadipole contributions, as well as interactions between terms of the same symmetry. Linear dichroism would result from a change in relative weights of these spectral components with orientation.

3.1 MnO

Momentum-transfer-dependent data for a pressed-powder sample of MnO are shown in figure 2. Data taken at 1.4 $Å^{-1}$ and 4.6 $Å^{-1}$ involved analyzers with 0.9 eV resolution. The behaviour for the Mn $M_{2,3}$ edges is similar to that for cerium in that the dipole feature at low q peaks, then diminishes and is replaced with increasing q by a feature at lower energy loss. The high-q feature covers a significantly smaller energy range than the features for the Ce 4d edges and is less well-separated (3.5 eV versus 10 – 15 eV peak to peak). There is an apparent peak shift in the octupole region of the spectrum which is likely due to the interaction between T_{1u} terms in the dipole and octupole components. We focus our treatment on the high-q regime to examine the dichroism in the octupole feature.

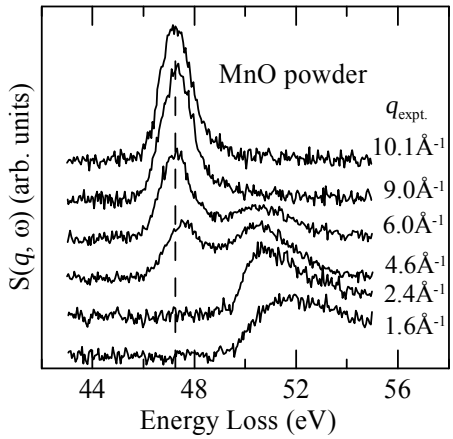

Figure 2. Contribution to S(q, ω) from the 3p initial states for a powder sample of MnO showing the effect of increasing momentum transfer on the XRS spectrum. The vertical dashed line is at 47.25 eV.

Two crystal substrate surfaces with (100) and (111) orientations were examined with 0.55eV resolution at 9.8 and 10.1 $Å^{-1}$, respectively (**q** parallel to the surface normal to within 1°, measured at different times with different LERIX configurations). In the initial model, based on the local many-body multiplet approach used for the *d-d* excitations in NiO and CoO [13] but, again, including core hole effects, the individual spectral components were calculated, figure 3a. A lifetime broadening of

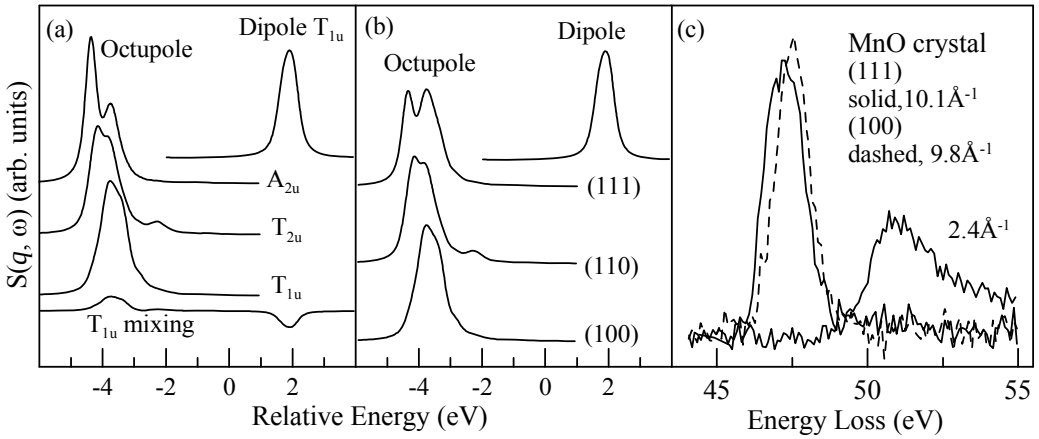

Figure 3. Comparison of theory and experiment for two orientations of single crystal MnO showing (a) spectral components and (b) calculated orientation dependence for 10$Å^{-1}$ along with (c) experimental results for (111) and (100) orientations.

0.3 eV has been factored in to the calculations. Calculated contributions, based on relative weights of the components, for the (100), (110) and (111) directions are shown in figure 3b. In this initial model, the (111) direction is readily distinguished from the other orientations by a difference in structure. The measured XRS spectra for (111) and (100) orientations are given in figure 3c along with a measurement of the (111) orientation at low q (2.4 $Å^{-1}$). While overall peak shape and apparent position differ for the two orientations, the calculated splitting in the (111) peak shown in figure 3b is not readily observed here. Broadening of multiplet features would obscure them and would be associated with experimental resolution being lower than optimal as well as additional decay channels beyond what is contained in the original cluster calculation. Including a Mn Auger MVV transition [19] which can mix with the $3p^5 3d^6$ final eigenstates, into the configuration mixing, along with the experimental resolution, brings the calculation into agreement with the data.

3.2. CeO_2

Cerium dioxide is a complicated system. While cerium is formally tetravalent in this compound, some mixing with oxygen 2p states occurs [20]. Debate exists over the extent of mixing between states with $4f^0$ and $4f^1\underline{L}$ ($\underline{L}$=ligand hole) character [21-25] leading to controversy in the picture of the local electronic initial state of Ce in CeO_2. The non-dipole multiplets observed in XRS measurements [14] resemble those for $4d^9 4f^1$ final state, but with some broadening. This is similar to what is observed in the soft x-ray work at the Ce $N_{4,5}$ edges [25]. Measurements of the multiplet spectrum for 3 separate orientations - (100), (110) and (111) - were done for a q of 10.1 $Å^{-1}$ and are compared in figure 4.

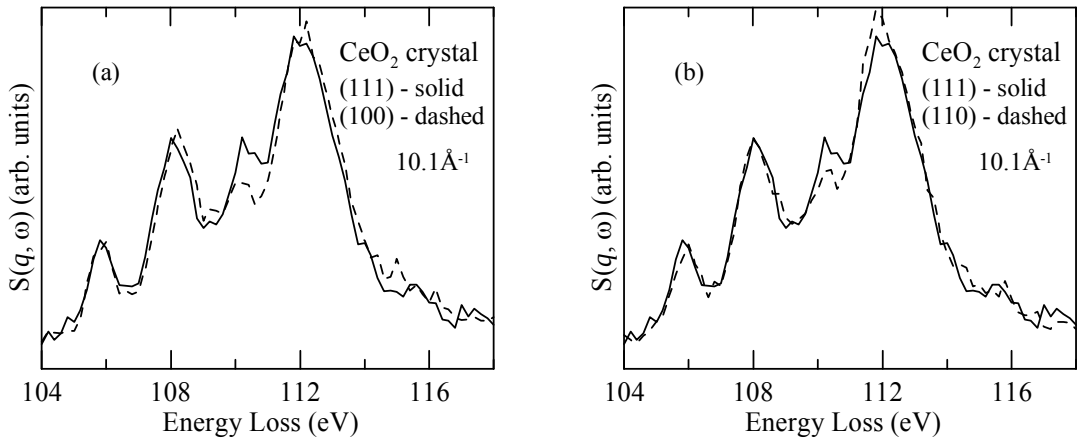

Figure 4. Comparison of (a) (111) and (100) orientations and (b) (111) and (110) orientations for single-crystal CeO_2 at 10.1$Å^{-1}$.

Cerium dioxide does exhibit dichroism at high-q. Peaks that first appear in the octupole term at intermediate q (figure 1) exhibit an apparent shift for the (100) orientation of ~ 0.15 – 0.2 eV higher than for (111) or (110). The (110) orientation does not appear shifted relative to (111) but, like the (100) orientation, is significantly lower in intensity near 111 eV. The lowest energy peak does not noticeably shift between the three orientations. Initial calculations within a purely atomic crystal-field multiplet approach, and for a purely $4f^0$ system do not show any substantial dichroism for any reasonable values of parameters. Since the 4f states only weakly interact with the CF, final state CF effects are found to contribute only negligibly to the dichroism. That a noticeable dependence is observed may be a direct measurement of the interaction leading to the mixed $4f^0$-$4f^1\underline{L}$ character. Efforts to better understand this behavior are ongoing.

In summary, we have measured XRS spectra and pursued efforts at modelling natural dichroism in cubic MnO and CeO_2 at high momentum transfer. For MnO, calculation based on methods used to model NiO and CoO *d-d* excitations were more involved, requiring the inclusion of additional final-

state mixing with Mn Auger-related states. Dichroism is evident in the high-*q* multiplet features of CeO_2. Modelling efforts are more challenging however due to uncertainty in the type and extent of configuration mixing.

Acknowledgements
This work was supported by grants from NSERC of Canada, the Canadian Institute for Advanced Research, the Max Planck Society and a grant from the D&LG Fund. We thank G.T. Seidler, S. Adler (U.Washington) and M. Urbanik (Comm. Crys. Labs.) for advice on LERIX and heat-treating CeO_2; Q. Qian (NJ-XRSTech) for analyzer tests and I.M. Chou for the MnO powder sample. PNC/XOR facilities at the Advanced Photon Source are supported by the US Department of Energy - Basic Energy Sciences, a Major Resources Support grant from NSERC, the University of Washington, Simon Fraser University and by the Advanced Photon Source under contract DE-AC02-06CH11357.

References
[1] Dräger G, Frahm R, Materlik G and Brümmer O 1988 *Phys. Stat. Sol.* B **146** 287
[2] Tohji K, Udagawa Y, Matsushita T, Nomura, M and Ishikawa T, 1990 *J. Chem. Phys.* **92** 3233
[3] van der Laan G, Schofield P F, Cressey G and Henderson C M B 1996 *Chem. Phys. Lett.* **252** 272
[4] Heumann D, Dräger G and Bocharov S 1997 *J. Phys. IV France* C2 **7** 481
[5] Cabaret D, Brouder C, Arrio M-A, Sainctavit P, Joly Y, Rogalev A and Goulon J 2001 *J. Synchrotron Rad.* **8** 460
[6] Juhin A, Brouder C, Arrio M-A, Cabaret D, Sainctavit P, Balan E, Bordage A, Seitsonen A P, Calas G, Eeckhout S G and Glatzel P 2008 *Phys. Rev. B.* **78** 195103
[7] For example: Chalmin E, Farges F and Brown G E Jr, 2009 *Contrib. Mineral Petrol.* **157** 111 and references therein
[8] Zhang G P and Callcott T A 2006 *Phys. Rev. B.* **73** 125102
[9] Huotari S, Pylkkänen T, Vankó G, Verbeni R, Glatzel P and Monaco G 2008 *Phys. Rev. B.* **78** 41102 R
[10] Nakai S, Ohkawa K, Takada Y, Odaka M, Kashiwakura T and Yamazaki T 2004 *J. Electr. Spectr. Rel. Phenom.* **137-140** 363
[11] Pettifer R F, Collins S P and Laundy D, 2008 *Nature* **454** 196
[12] Larson B C, Wei K, Tischler J Z, Lee C-C, Restrepo O D, Eguiluz A G, Zschack P and Finkelstein K D 2007 *Phys. Rev. Lett.* **99** 26401
[13] Haverkort M W, Tanaka A, Tjeng L H and Sawatzky G A 2007 *Phys. Rev. Lett.* **99** 257401
[14] Gordon R A, Seidler G T, Fister T T, Haverkort M W, Sawatzky G A, Tanaka A and Sham T K 2008 *Europhys. Lett.* **81** 26004
[15] Soininen J A, Ankudinov A L and Rehr J J 2005 *Phys. Rev. B* **72** 045136
[16] Chou I-M 1978 *Am. Mineral.* **63** 690
[17] Fister T T, Seidler G T, Wharton L, Battle A R, Ellis T B, Cross J O, Macrander A T, Elam W T, Tyson T A and Qian Q 2006 *Rev. Sci. Instr.* **77** 63901
[18] Altmann S L and Cracknel A P 1965 *Rev. Mod. Phys.* **37** 19
[19] Sundaramoorthy R, Weiss A H, Hulbert S L and Bartynski R A 2008 *Phys. Rev. Lett.* **101** 127601
[20] Mullins D R, Overbury S H and Huntley D R, 1998 *Surf. Sci.* **409** 307
[21] Nakazawa M, Ogasawara H and Kotani A, 2000 *J. Phys. Soc. Japan* **69(12)** 4071
[22] Loschen C, Carrasco J, Neyman K M and Illas F, 2007 *Phys. Rev. B* **75** 35115
[23] Hague C F, Mariot J-M, Delaunay R, Gallet J-J, Journel L and Rueff J-P, 2004 *J. Electr. Spectr. Rel. Phenom.* **136** 179
[24] Skorodumova N V, Ahuja R, Simak S I, Abrikosov I A, Johansson B and Lundqvist B I, 2001 *Phys. Rev. B* **64** 115108
[25] Jo T and Kotani A, 1988 *Phys. Rev. B* **38** 830